Simultaneous measurement of temperature and refractive index based on a core-offset Mach-Zehnder interferometer cascaded with a long-period fiber grating*

CAO Ye (曹晔), **LIU Hui-ying** (刘慧莹)**, **TONG Zheng-rong** (童峥嵘), **YUAN Shuo** (袁硕), **and ZHAO Shun** (赵舜)

Key Laboratory of Film Electronics and Communication Devices, Tianjin University of Technology, Tianjin 300384, China

(Received 3 July 2014)

An all-fiber sensor based on a cascaded optical fiber device is proposed and demonstrated, and its sensor head is composed of a core-offset Mach-Zehnder interferometer (MZI) and a long-period fiber grating (LPFG). In the experiment, two dips shaped by the intermodulation between the interference fringe of MZI and the resonant wavelength of LPFG are monitored. Experimental results show that temperature sensitivities of two dips are 0.060 7 nm/°C and 0.056 3 pm/°C, and the refractive index (RI) sensitivities are –18.025 nm/RIU and –55.06 nm/RIU, respectively. The simultaneous measurement of the temperature and external RI is demonstrated based on the sensitive matrix. Its low fabrication cost, simple configuration and high sensitivity make this sensor have potential applications in chemical and biological sensing.

Document code: A **Article ID:** 1673-1905(2015)01-0069-4

DOI 10.1007/s11801-015-4127-x

Fiber sensors are widely used in sensing measurement fields, such as temperature, strain, micro-displacement and refractive index, because of their unique advantages of small size, light weight, immunity to electromagnetic interference, resistance to high pressure and high temperature, corrosion-resistance and so on[1-3].

Optical fiber sensors based on interference principle have the advantages of high sensitivity and flexible structure. In recent years, various on-line optical fiber interferometric sensors have been reported, such as single mode-multimode-single mode (SMS) structure[4], single-mode fiber cascaded with thin-core fiber[5], tapered fiber or peanut-shape Mach-Zehnder interferometer (MZI)[6], laser drilling and core-offset splicing[7]. In 2012, Liu et al[8] proposed a single mode-multimode-thin core multimode-single mode (SMTMS) sensor to achieve simultaneous measurement of the temperature and the refractive index (RI). The low-cost structure has high practical value, but the sensitivity needs to be improved. In 2014, Dong et al[9] proposed a highly sensitive micro-displacement sensor based on MZI by a bowknot type taper. The intensity demodulation method is used to avoid the influence of temperature, and a higher sensitivity is obtained experimentally.

In addition, some scholars embeded fiber gratings into the above interferometers to achieve a composite parameter sensing by simultaneously monitoring the resonant wavelengths of both fiber grating and interferometer. In 2013, Zhang[10] proposed a cascaded optical fiber device composed of a long-period fiber grating (LPFG) and an S-type fiber taper MZI (SFT-MZI). The crosstalk problem is solved because different resonance peaks of LPFG and MZI possess different RI and temperature sensitivities. In 2014, Meng[11] proposed a new-type sensor which contains a core-offset MZI and a fiber Bragg grating (FBG). The interference fringe of MZI and the Bragg wavelength of FBG would shift with the variation of ambient RI and temperature. The structure has some advantages, such as low fabrication cost and simple configuration, but its sensitivity still needs to be improved.

LPFG has been widely used in optical fiber sensing and optical fiber communication because of its low insertion loss, wide bandwidth and high sensitivity in response to the external environment[12]. Even so, LPFG still has some drawbacks, such as the discrimination of the cross-sensitivity between the surrounding refractive index (SRI) and temperature. Therefore, LPFG and core-offset MZI are combined in this paper. The interference fringe of MZI and the resonance peak of LPFG

* This work has been supported by the National High Technology Research and Development Program (No.2013AA014200), the National Natural Science Foundation of China (No.61107052), the Natural Science Foundation of Tianjin (No.14JCYBJC16500), and the Tianjin University's Science and Technology Development Fund Projects (No.2012).

** E-mail: winnerhuiying@163.com

possess different temperature and RI sensitivities, so the simultaneous measurement of temperature and RI can be achieved. The design is simple and low cost, and the introduction of LPFG improves the sensitivity of sensor.

The experimental device is shown as Fig.1. The light emitted from the broadband light source (BBS) is transferred into single mode fiber (SMF), and then the interference is formed by the mode coupling when light passes through the sensor head. Finally, these modes are transmitted to optic spectrum analyzer (OSA) through the SMF.

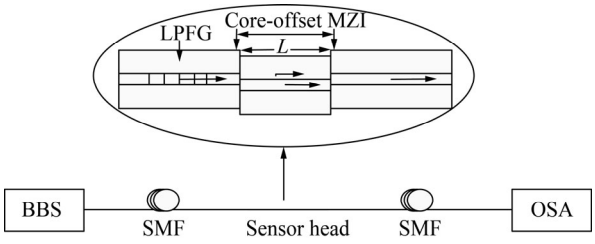

Fig.1 Schematic diagram of the experimental device

By offsetting two SMF cores by several micrometers (usually less than 9 μm), a common design as shown in Fig.2 can achieve fixed attenuation.

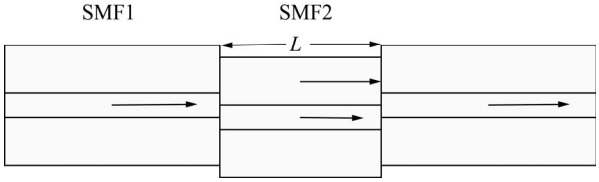

Fig.2 Structure of the core-offset MZI

According to the conservation of energy[13], the light from the transmission fiber (SMF1) is split into two paths. One path is coupled to the core mode of the sensing SMF2, while the other path is transferred to the cladding and subsequently propagates as cladding modes. Owing to the attenuation at the interface of cladding and coating, the cladding modes cannot propagate over a long distance. In this case, another core offset of only several centimeters is introduced after the first one, so the light in the cladding can be recoupled to the core with ignorable loss. Due to the phase difference of cladding and core modes, an MZI is realized by the second offset.

In the core-offset structure[14], the strongest interference occurs between the fiber core mode and the dominant cladding mode. The phase difference between the core mode and the cladding mode is

$$\phi = 2\pi\Delta nL / \lambda , \tag{1}$$

where Δn is the effective index difference between core and cladding, λ is the wavelength in vacuum, and L is the length of interferometer arm SMF2. The wavelength of maximum interference is

$$\lambda_{\text{core-offset}} = \frac{\lambda^2}{\Delta nL} . \tag{2}$$

When environmental temperature or RI is varied, Δn and L will be changed. Consequently, wavelength shift of the interference pattern will occur, and then the variation of RI and temperature can be monitored.

In a standard LPFG[15], according to the coupled mode theory, the phase matching between the core mode and the m-order forward-propagating cladding mode is achieved at resonant wavelengths, which can be given as

$$\lambda_{\text{LPFG}} = (n_{\text{eff}}^{\text{co}} - n_{\text{eff}}^{\text{cl},m})\Lambda , \tag{3}$$

where $n_{\text{eff}}^{\text{co}}$ and $n_{\text{eff}}^{\text{cl},m}$ are the effective refractive indices of the core and the m-order cladding mode, respectively, Λ is the period of LPFG, and λ_{LPFG} is the resonance wavelength of LPFG.

When the temperature is changed by ΔT and the refractive index varies from n_1 to n_2, the resonance wavelength of LPFG is changed by

$$\Delta\lambda = \left[\left(n_{\text{eff}}^{\text{co}} - n_{\text{eff}}^{\text{cl},m} \right) \frac{\mathrm{d}\Lambda}{\mathrm{d}T} + \left(\frac{\mathrm{d}n_{\text{eff}}^{\text{co}}}{\mathrm{d}T} - \frac{\mathrm{d}n_{\text{eff}}^{\text{cl},m}}{\mathrm{d}T} \right) \Lambda \right] \Delta T + \frac{U_\infty \Lambda}{n_{\text{cl}} b^3 k^3} \left(\frac{1}{\sqrt{n_{\text{cl}}^2 - n_1^2}} - \frac{1}{\sqrt{n_{\text{cl}}^2 - n_2^2}} \right) , \tag{4}$$

where b is the radius of the cladding, n_{cl} is the refractive index of the cladding, and U_∞ is the m-order root of J_0 which is the zero-order Bessel function of the first kind.

It can be concluded that the interference fringe of MZI and the resonance wavelength of LPFG have different sensitivities of RI and temperature. As a result, simultaneous measurement of RI and temperature can be realized by using sensitive matrix.

As the experimental arrangement shown in Fig.1, a BBS and an OSA (MS9710b) with a wavelength resolution of 0.07 nm are used. The SMF is made by YOFC, where diameters of core and cladding are 8.3 μm and 125 μm, respectively. The LPFG used in our experiment is written by CO_2 laser. The grating pitch is 620 μm, and the length of the grating is 3.72 cm. The length of core offset is 4 cm, and the offset is about 4 μm. Then combine the MZI with LPFG. The transmission spectra of the cascaded device in pure water at room temperature are shown in Fig.3.

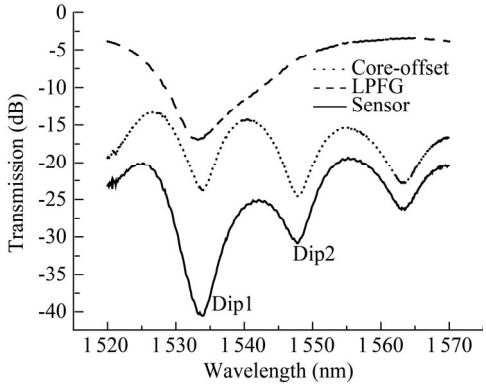

Fig.3 Transmission spectra of core-offset MZI, LPFG and cascaded sensor in pure water at room temperature

As shown in Fig.3, the interference spectrum of MZI is modulated by LPFG. Therefore, three resonance peaks are displayed around the resonance peak of LPFG. Dip1 (1 533.9 nm) and Dip2 (1 547.8 nm) which are close to the resonance peak of LPFG are selected to be monitored when considering the precision of measurement result. The two resonance peaks are formulated by intermodulation between LPFG and MZI, so they have the sensitive features of the two structures when outside parameters change.

Fig.4 shows the schematic diagram of the temperature characteristic experiment. For the temperature measurement, the sensor head is fixed in the pure water. The water temperature changes from high (75 °C) to low (25 °C) to avoid bending caused by thermal expansion. Mercury thermometer is used to read the value of temperature. The shifts of two dips are recorded every 5 °C. The output spectra at 25 °C and 75 °C are shown in Fig.5(a). After test, the temperature response characteristic curves for two dips are achieved as shown in Fig.5(b). It can be seen that the two dips both show blue shift with the decrease of temperature. So, when temperature increases, Dip1 and Dip2 both move towards longer wavelength linearly, and the temperature sensitivities of Dip1 and Dip2 are 0.060 7 nm/°C and 0.056 3 nm/°C, respectively.

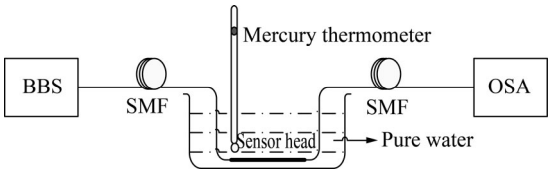

Fig.4 Schematic diagram of the temperature characteristic experiment

Fig.6 shows the schematic diagram of the refractive index characteristic experiment. To get the RI sensitivity of the sensor, we use a commercial Abbe refractometer. By increasing the concentration of NaCl, liquid samples with refractive indices varying from 1.33 to 1.38 are obtained. Then the sensor head is placed into the NaCl solution. Fig.7(a) shows the output spectra of liquid samples with refractive indices of 1.33 and 1.38, and Fig.7(b) shows the RI responses of the sensor head. Obviously, a blue shift happens to both two dips when RI increases. The fitting results show that the shift is linear, and the RI sensitivities of Dip1 and Dip2 are –18.025 nm/RIU and –55.06 nm/RIU, respectively.

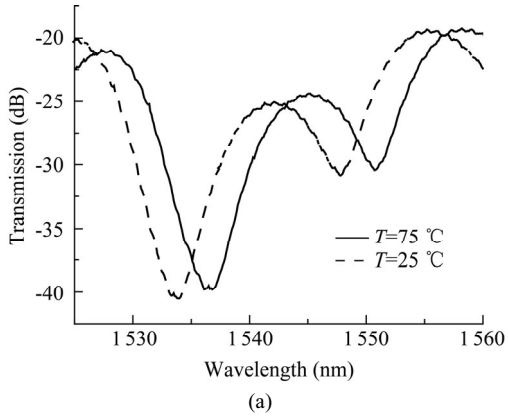

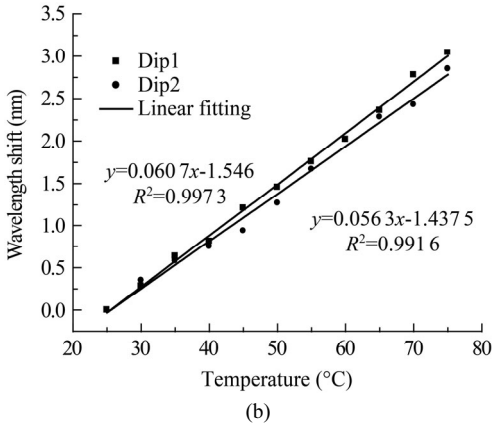

Fig.5 (a) Output spectra at 25 °C and 75 °C; (b) Temperature response characteristic curves

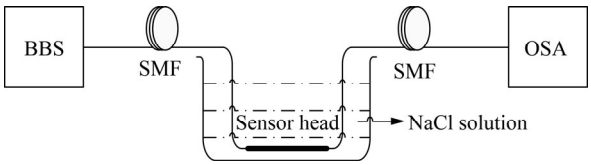

Fig.6 Schematic diagram of the refractive index characteristic experiment

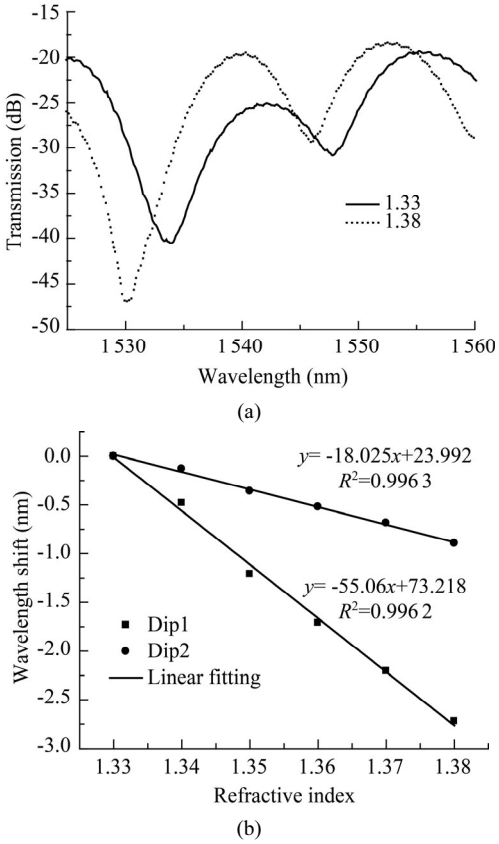

Fig.7 (a) Output spectra of solutions with refractive indices of 1.33 and 1.38; (b) Refractive index response curves

It can be concluded from the measurement results of the above experiments that the sensitivity coefficients are

different when the shifts of Dip1 and Dip2 are controlled by temperature and RI. The responses of the sensor to RI and temperature can be expressed in matrix form as

$$\begin{bmatrix}\Delta\lambda_1\\ \Delta\lambda_2\end{bmatrix}=\begin{bmatrix}K_{T1} & K_{n1}\\ K_{T2} & K_{n2}\end{bmatrix}\begin{bmatrix}\Delta T\\ \Delta n\end{bmatrix}, \tag{5}$$

where $\Delta\lambda_1$ and $\Delta\lambda_2$ are the shifts of Dip1 and Dip2, respectively, ΔT is the change of temperature, Δn is the change of RI, K_{T1} and K_{n1} are the thermal coefficient and RI coefficient of Dip1, and K_{T2} and K_{n2} are the thermal coefficient and RI coefficient of Dip2, respectively.

According to the two separate temperature and RI measurements, the sensor matrix can be obtained as

$$\begin{bmatrix}\Delta T\\ \Delta n\end{bmatrix}=\frac{1}{D_1}\begin{bmatrix}K_{n2} & -K_{n1}\\ -K_{T2} & K_{T1}\end{bmatrix}\begin{bmatrix}\Delta\lambda_1\\ \Delta\lambda_2\end{bmatrix}, \tag{6}$$

where $D_1=K_{T1}K_{n2}-K_{T2}K_{n1}$.

Then substitute the experimental data into Eq.(6) and get

$$\begin{bmatrix}\Delta T\\ \Delta n\end{bmatrix}=\frac{1}{-2.32}\begin{bmatrix}-55.06 & 18.025\\ -0.056\,3 & 0.060\,7\end{bmatrix}\begin{bmatrix}\Delta\lambda_1\\ \Delta\lambda_2\end{bmatrix}. \tag{7}$$

Therefore, the cascaded device composed of LPFG and core-offset MZI can be used to measure the changes of the liquid's temperature and refractive index simultaneously.

In conclusion, an all-fiber sensor device composed of core-offset MZI and LPFG is developed and investigated for simultaneously measuring temperature and RI. In the experiment, we select two different dips in the transmission spectrum formed by the intermodulation between LPFG and core-offset MZI, and then get the temperature sensitivities of 0.607 nm/°C and 0.056 3 nm/°C and the RI sensitivities of –55.06 nm/RIU and –18.025 nm/RIU, respectively. Experimental results confirm the feasibility of this design. The whole experimental system has high sensitivity, simple structure and low cost, which makes the proposed cascaded device be used in various applications.

References

[1] OU Qi-biao, ZENG Qing-ke, QING Zi-xiong and LI Chuan-qi, Journal of Optoelectronics·Laser **24**, 323 (2013). (in Chinese)

[2] Jie Shi, Shilin Xiao, Miehua Bi, Lilin Yi and Pei Yang, Applied Optics **51**, 2733 (2012).

[3] SHI Sheng-hui, ZHOU Xiao-jun, ZHANG Zhi-yao and LIU Yong, Journal of Optoelectronics·Laser **23**, 1644 (2012). (in Chinese)

[4] Qiang Wu, Yuliya Semenova, Pengfei Wang and Gerald Farrell, Optics Express **19**, 7937 (2011).

[5] Jiangtao Zhou, Yiping Wang, Changrui Liao, Guolu Yin, Xi Xu, Kaiming Yang, Xiaoyong Zhong, Qiao Wang and Zhengyong Li, IEEE Photonics Technology Letters **26**, 508 (2014).

[6] Huaping Gong, Xiao Yang, Kai Ni, Chun-Liu Zhao and Xinyong Dong, IEEE Photonics Technology Letters **26**, 22 (2014).

[7] Zhaobing Tian, Scott S.-H. Yam and Hans-Peter Loock, IEEE Photonics Technology Letters **20**, 1387 (2008).

[8] Lecheng Li, Xia Li, Zhenhai Xie, Zhaolong Liao, Feng Tu and Deming Liu, Optics Communications **285**, 3945 (2012).

[9] Chang-Yu Shen, Jin-Lei Chu, Yan-Fang Lu, De-Bao Chen, Chuan Zhong, Yi Li, Xin-Yong Dong and Shang- Zhong Jin, IEEE Photonics Technology Letters **26**, 62 (2014).

[10] Jieliang Li, Weigang Zhang, Shecheng Gao, Pengcheng Geng, Xiaolin Xue, Zhiyong Bai and Hu Liang, IEEE Photonics Technology Letters **25**, 888 (2013).

[11] Qiqi Yao, Hongyun Meng, Wei Wang, Hongchao Xue, Rui Xiong, Ben Huang, Chunhua Tan and Xuguang Huang, Sensors and Actuators A: Physical **209**, 73 (2014).

[12] Zhengtian Gu, Xiuli Jiang and Haiyun Chen, Optical Engineering **53**, 021104 (2014).

[13] Zhaobing Tian and S. S.-H. Yam, Journal of Lightwave Technology **27**, 2296 (2009).

[14] Lili Mao, Ping Lu, Zefeng Lao, Deming Liu and Jiangshan Zhang, Optics & Laser Technology **57**, 39 (2014).

[15] HU Xing-liu, LIANG Da-kai, FANG Ting, WANG Yan and LI Dan, Journal of Optoelectronics·Laser **23**, 1659 (2012). (in Chinese)